^{239}Pu nuclear magnetic resonance in the candidate topological insulator PuB_4

A. P. Dioguardi,[1,2,*] H. Yasuoka,[1,3] S. M. Thomas,[1] H. Sakai,[1,4] S. K. Cary,[1] S. A. Kozimor,[1] T. E. Albrecht-Schmitt,[5] H. C. Choi,[1] J.-X. Zhu,[1] J. D. Thompson,[1] E. D. Bauer,[1] and F. Ronning[1]

[1]*Los Alamos National Laboratory, Los Alamos, New Mexico 87545, USA*

[2]*IFW Dresden, Institute for Solid State Research, P.O. Box 270116, D-01171 Dresden, Germany*

[3]*Max Planck Institute for Chemical Physics of Solids, 01187 Dresden, Germany*

[4]*Advanced Science Research Center, Japan Atomic Energy Agency, Tokai, Naka, Ibaraki 319-1195, Japan*

[5]*Department of Chemistry and Biochemistry, Florida State University, 95 Chieftan Way, Tallahassee, Florida 32306, USA*

(Received 15 August 2018; published 2 January 2019)

We present a detailed nuclear magnetic resonance (NMR) study of ^{239}Pu in bulk and powdered single-crystal plutonium tetraboride (PuB_4), which has recently been investigated as a potential correlated topological insulator. This study constitutes the second-ever observation of the ^{239}Pu NMR signal, and provides unique on-site sensitivity to the rich f-electron physics and insight into the bulk gaplike behavior in PuB_4. The ^{239}Pu NMR spectra are consistent with axial symmetry of the shift tensor showing for the first time that ^{239}Pu NMR can be observed in an anisotropic environment and up to room temperature. The temperature dependence of the ^{239}Pu shift, combined with a relatively long spin-lattice relaxation time (T_1), indicate that PuB_4 adopts a nonmagnetic state with gaplike behavior consistent with our density functional theory calculations. The temperature dependencies of the NMR Knight shift and T_1^{-1}–microscopic quantities sensitive only to bulk states–imply bulk gaplike behavior confirming that PuB_4 is a good candidate topological insulator. The large contrast between the ^{239}Pu orbital shifts in the ionic insulator PuO_2 ($\sim$+24.7%) and PuB_4 ($\sim$−0.5%) provides a new tool to investigate the nature of chemical bonding in plutonium materials.

DOI: 10.1103/PhysRevB.99.035104

Topological insulators have received much attention recently due to the experimental verification of the theoretical prediction of topologically nontrivial symmetry-protected surface states [1,2]. Kondo insulators are f-electron systems with strong correlations in which hybridization of the f electrons with conduction electrons forms a gap at the Fermi level [3]. Strong spin-orbit coupling can result in a topological Kondo insulator in which band inversion drives the emergence of nontrivial topologically protected gapless surface states [4,5]. Samarium hexaboride (SmB_6) is the primary candidate example of a topological Kondo insulator [6–9]. As compared with rare-earth $4f$-electron systems, the actinide $5f$-electron systems have more spatially extended f-electron wave functions, which generally results in an enhancement of the energy scales involved [10–12]. Plutonium (Pu) materials display particularly complex physical properties due to the $5f$ electrons lying on the brink between bonding and nonbonding configurations [13,14]. For example, elemental Pu forms in six allotropes at ambient pressure that vary in density by up to 25% [15,16]. Pu compounds display a wide variety of electronic ground states including heavy-fermion behavior, magnetism, superconductivity [17], and most recently the prediction of topologically nontrivial states [12,18].

Very recently, plutonium tetraboride (PuB_4) has been theoretically predicted to be a strong topological insulator in which electronic correlations play an important role [19]. The density functional theory (DFT) calculations predict a band gap $\Delta \sim 254$ meV and dynamical mean-field theory (DMFT) calculations find that electronic correlations significantly reduce the magnitude of the predicted energy gap. Experimental measurements from the same work find an increase of the resistivity with decreasing temperature and saturation at low temperature reminiscent of the behavior of SmB_6 [20]. Fits to the temperature-dependent resistivity yield an energy gap $\Delta = 35$ meV, which is taken as evidence for correlation-induced suppression of the expected gap value. PuB_4 forms in the tetragonal ThB_4-type crystal structure with space group *P4/mbm* (# 127) as shown in Fig. 1(a) and was first reported nearly 60 years ago [21–23]. Magnetic measurements of PuB_4 indicated that the Pu magnetic moment is very small, on the order of 7.2×10^{-4} emu/mol and shows little temperature dependence [24]. This small magnetic susceptibility and insulatinglike electrical transport make PuB_4 an ideal material in which to search for ^{239}Pu nuclear magnetic resonance (NMR).

NMR is a powerful tool for the investigation of the physics and chemistry of condensed matter in general [26–29]. The ^{239}Pu nucleus has nuclear spin $I = \frac{1}{2}$ and is of great interest as an on-site probe of the rich f-electron physics of Pu. The first attempt to observe ^{239}Pu NMR was performed on α-Pu more than 50 years ago [30], however, to date there is only a single report of ^{239}Pu NMR [31] in the ionic insulator PuO_2. The main difficulty involved in observing ^{239}Pu NMR, and other f-electron nuclei, in general, can be traced to the very strong hyperfine fields at the nucleus produced by on-site hyperfine coupling to the f electrons. Consequently, the resulting spectral width can be very large, and the spin-lattice (T_1) and spin-spin (T_2) relaxation times can be extremely short, which

*adioguardi@gmail.com

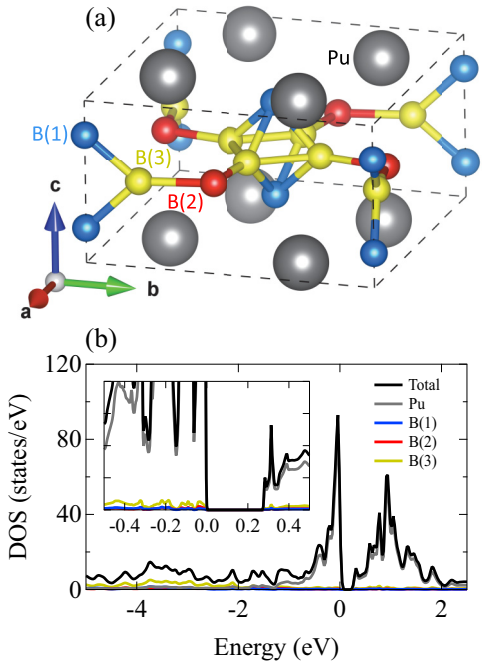

FIG. 1. (a) Unit cell of PuB_4 illustrating the single plutonium site and three inequivalent boron sites [25]. (b) Density of states (DOS) and partial DOS as a function of energy calculated within density functional theory including spin-orbit coupling. The inset shows an expanded region near the Fermi energy where there is an energy gap of $\Delta \sim 254$ meV.

makes detection of the signal difficult. These effects can be minimized in systems with a gap in the electronic and spin excitation spectrum, as evident in the case of PuO_2, UO_2, and YbB_{12} [31–33].

Here we report the observation of, and the microscopic properties extracted from, ^{239}Pu NMR in powdered and single crystalline PuB_4. Crystals were grown by an Al-flux method and sample preparation details are provided in the Supplemental Material [34]. We deduce the resonant condition of ^{239}Pu in PuB_4 $^{239}\gamma(1 + K_{PuB4})/2\pi = 2.288 \pm 0.001$ MHz/T from the powder spectra, and find axial symmetry of the hyperfine interaction on the Pu site. Both the powder and the single-crystal Knight shift $K(T)$ of ^{239}Pu show temperature dependence consistent with gaplike behavior with a static energy gap [extracted from the single crystalline $K_c(T)$ data] $\Delta_K \approx 156$ meV. The relaxation time is quite long—on the order of milliseconds to seconds—even at the ^{239}Pu site, indicating that the f-electron configuration is nonmagnetic. The dominant temperature dependence of the spin-lattice relaxation rate $T_1^{-1}(T)$ also shows gaplike behavior with a dominant dynamic gap $\Delta_{T_1} \approx 251$ meV. We compare our experimental NMR results with the density of states, calculated within density functional theory including spin-orbit coupling, which finds a gap of similar order of magnitude. A weak low-temperature peak in $T_1^{-1}(T)$ indicates the presence of bulk in-gap magnetic states with a gap $\delta \approx 2$ meV.

Our DFT calculations including spin-orbit coupling reveal a gap in the density of states (DOS) at the Fermi energy E_F of roughly 254 meV as shown in Fig. 1(b). To account for the presence of correlations we also performed DFT + DMFT calculations. Using a U of 4.5 eV and high-order Slater integrals amounting to an effective $J = 0.512$ eV [35,36] and attempting to stabilize a magnetic solution, we find that the self-consistent solution recovers a nonmagnetic state with a band gap at the Fermi level of order 10.3 meV (see Supplemental Material for further calculation details [34]). The appreciable calculated gap in the DOS combined with an expected nonmagnetic ground state indicate the probable absence of strong spin- and charge-relaxation channels, and therefore, we expect the spin-lattice relaxation rate in PuB_4 to be long enough to observe the ^{239}Pu signal. The ^{239}Pu nucleus has $I = \frac{1}{2}$ and the bare gyromagnetic ratio was determined based on the initial observation in PuO_2 to be $^{239}\gamma/2\pi = 2.29 \pm 0.001$ MHz/T [31]. Consequently, we would expect to find an NMR signal in the field range of roughly 7–9 T with an rf excitation frequency $f_0 \sim 20$ MHz. Indeed, for $f_0 = 20.222$ MHz we discovered an asymmetric powder spectrum between 8.80 and 8.92 T as shown in Figs. 2(a)–2(b). To establish that the observed signal is indeed due to ^{239}Pu from PuB_4 field-swept spectra were collected at several frequencies. These spectra are shown in Fig. 2(a) and they confirm the intrinsic nature of the NMR signal.

The crystal structure of PuB_4 has a single Pu site with oriented site symmetry *m.2m* [see Fig. 1(a)]. For each crystallite in the powdered sample the resonance condition can be expressed as $2\pi f_0 = \gamma B_0(1 + K_i)$ where K_i are the elements of the shift tensor for a given field orientation and B_0 is the magnetic field at which the resonance occurs for frequency f_0. Although the local symmetry is orthorhombic in principle, the nonaxial components of the shift tensor are found to be extremely close to zero from the spectral pattern in Fig. 2(b), i.e., it can be practically regarded to be tetragonal. Assuming tetragonal symmetry for the hyperfine interaction on Pu, the isotropic and axial shifts (K_{iso} and K_{ax}, respectively) are extracted from the observed K_c and K_{ab} using $K_{iso} = (K_c + 2K_{ab})/3$ and $K_{ax} = (K_c - K_{ab})/3$, where the angular dependence of the shift is given by $K(\theta) = K_{iso} + K_{ax}(3\cos^2\theta - 1)$.

The isotropic shift of ^{239}Pu in PuB_4 is $K_{iso}(T = 4\,\mathrm{K}) = -0.09 \pm 0.04\%$ is obtained from the slope in the frequency vs field plot in Fig. 2(a). This value is notably different from the shift $K(T = 4\,\mathrm{K}) = 24.72 \pm 0.04\%$ of ^{239}Pu in PuO_2 [31]. To calculate these shifts we have assumed the bare $^{239}\gamma/2\pi = 2.29$ MHz/T as determined from the study of PuO_2 [31]. $K_{ax}(T = 4\,\mathrm{K}) = -0.48 \pm 0.01\%$ is also significantly different from the shift found in PuO_2 [31] at the same temperature. It is worth noting that the relatively small absolute value of K_{ax} was crucial to find the ^{239}Pu signal in an anisotropic environment.

The temperature dependence of the field-swept spectra at $f_0 = 20.222$ MHz and the corresponding least-squares fits are shown in Fig. 2(b). An axially symmetric shift tensor remains a good approximation for all temperatures measured. Figure 2(c) illustrates that K_{iso} has a small negative value with a positive temperature dependence, and K_{ax} has a larger negative value with a smaller temperature dependence relative to K_{iso}. In general, K_{iso} originates from the spin-polarized Fermi contact interaction and couples to the uniform spin susceptibility via the hyperfine interaction. K_{ax} may be dominantly

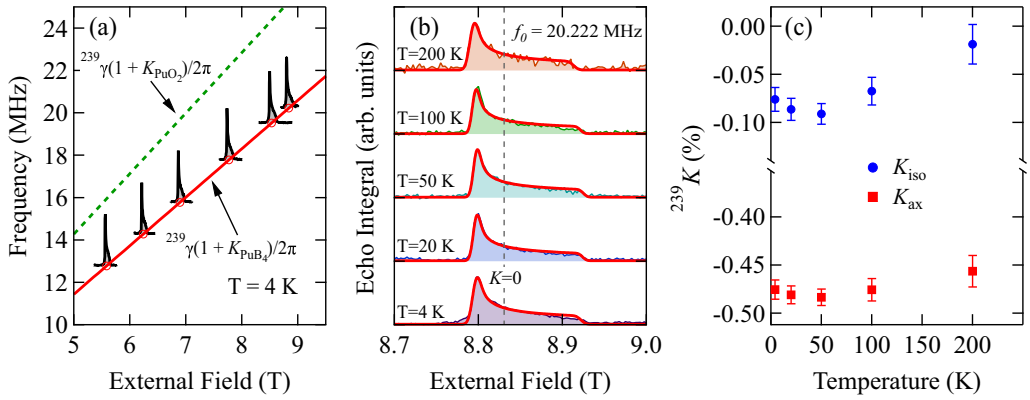

FIG. 2. (a) ^{239}Pu nuclear magnetic resonance (NMR) field-swept spectra of powdered single crystals of PuB_4 at several frequencies at $T = 4$ K. Spectra are normalized to the maximum value and offset vertically so as to correspond to the observed frequency f_0 on the left axis. Red circles and line indicate the resonant condition of ^{239}Pu in PuB_4 $^{239}\gamma(1 + K_{PuB_4})/2\pi = 2.288 \pm 0.001$ MHz/T (at $T = 4$ K) and green dashed line shows $^{239}\gamma(1 + K_{PuO_2})/2\pi = 2.856 \pm 0.001$ MHz/T as determine previously [31]. (b) ^{239}Pu NMR field-swept spectra at $f_0 = 20.222$ MHz offset vertically for several temperatures. Solid red curves are best fits as described in the text. Vertical dashed line indicates zero shift $K = 0$ using $^{239}\gamma/2\pi = 2.29$ MHz/T. (c) $^{239}K_{iso}$ and $^{239}K_{ax}$ vs temperature extracted from fits in (b).

attributed to the temperature-independent orbital hyperfine interaction with a small temperature dependence resulting from a reduction of the anisotropy of the spin susceptibility with increasing temperature. The facts that the spin-lattice relaxation time in PuB_4 is sufficiently long to enable the observation of ^{239}Pu NMR, and that Knight shifts are weakly temperature dependent imply that the electronic state of Pu in PuB_4 is nearly nonmagnetic. Assuming a local picture this implies either that Pu has a $5f^6$ configuration or PuB_4 adopts a Kondo insulating state.

Finally, we performed measurements on a single crystal of PuB_4 for the external field applied along the $\hat{c}$ axis. We measured both the $\hat{c}$-axis ^{239}Pu shift K_c and T_1^{-1} as a function of temperature up to 300 K as shown in Fig. 3. We fit the ^{239}Pu inversion recovery curves to the form

$$M_N(t) = M_N(\infty)\left(1 - \alpha e^{-(t/T_1)^\beta}\right), \tag{1}$$

where $M_N(\infty)$ is the equilibrium nuclear magnetization, α is the inversion fraction, T_1 is the spin-lattice relaxation time, and β is a stretching exponent that modifies the expected single exponential behavior ($\beta = 1$). We find that $\beta_{avg} = 0.813$, which is a measure of the width of the probability distribution of T_1 [37], is independent of temperature and may indicate sensitivity to self-irradiation-induced disorder [38]. Both K_c and T_1^{-1} are consistent with gaplike behavior, and T_1^{-1} exhibits a low-temperature maximum consistent with the presence of in-gap states, which are suppressed with applied magnetic field as shown in the inset of Fig. 3.

From a chemistry perspective, the ^{239}Pu orbital shift is very different between PuO_2 ($\sim$+24.7% [31]) and PuB_4 ($\sim$−0.5%). The origin of the difference in magnitude of the orbital shift is clear from the fact that in the case of PuO_2 the Pu ion has a completely ionic Pu^{4+} ($5f^4$) state and experiences strong cubic crystalline electronic field giving rise to a nonmagnetic ground state with a Van Vleck orbital magnetism, which is the main source of the hyperfine interaction to the Pu nuclear moment. In contrast, DFT + DMFT calculations point to PuB_4 being a strongly correlated insulator with possible strong topological character, similar to the case of SmB_6. In SmB_6 the gap arises from hybridization between $4f$ and ligand electrons that give rise to a pronounced nonintegral value of the $4f$ configuration. Our results suggest that this is also the case in PuB_4. The large difference in orbital shift between PuO_2 and PuB_4 clearly indicates that ^{239}Pu NMR is highly sensitive to the degree of bond mixing and the f-electron configuration. Furthermore, the relaxation time is roughly two orders of magnitude shorter than in PuO_2 [31], which likely reflects the difference in chemical environments between PuB_4 and PuO_2.

The capability to measure ^{239}Pu was key to observing gaplike behavior in the static and dynamic spin susceptibilities as evidenced by the temperature dependencies of K_c and T_1^{-1} shown in Fig. 3. Our ^{11}B measurements of the temperature dependence of the Knight shift (see Supplemental Material [34]) do not show any evidence of gaplike behavior, likely due to the much smaller value of the hyperfine coupling of the ^{11}B nuclei to the electrons as compared to the ^{239}Pu hyperfine coupling, which is expected to be on the order of 150 T/μ_B. Therefore, our ^{239}Pu NMR results are sensitive to otherwise enigmatic physics in PuB_4.

There exist a number of previous NMR studies that find gaplike behavior of f-electron systems, e.g., SmB_6 [39,40], YbB_{12} [33], $Ce_3Bi_4Pt_3$ [41]. Here we follow the analysis scheme of SmB_6 [40] by fitting the temperature dependence of the ^{239}Pu Knight shift and spin-lattice relaxation rate by assuming a simple model for the density of states near the Fermi energy. The Knight shift is given by,

$$K(T) \propto \int f(E,T)[1 - f(E,T)]\rho(E)dE, \tag{2}$$

where $f(E,T)$ is the Fermi function and $\rho(E)$ is the density of states. The spin-lattice relaxation rate is given by,

$$T_1^{-1}(T) \propto \int f(E,T)[1 - f(E,T)]\rho(E)^2 dE. \tag{3}$$

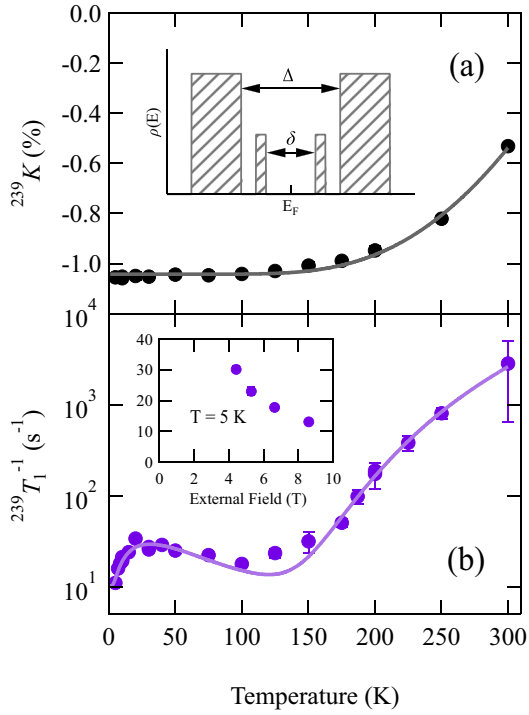

FIG. 3. Single-crystal ^{239}Pu NMR data for external field aligned along the crystalline $\hat{c}$ direction. (a) Shift K_c vs temperature and fit (solid line) to gaplike behavior as discussed in the text which yields an energy gap $\Delta_K = 155.6 \pm 11.0$ meV, but is not sensitive to the in-gap states. The inset shows the model density of states $\rho(E)$ vs energy E employed in the fits. (b) Spin-lattice relaxation rate T_1^{-1} vs temperature and fit (solid line) to gaplike behavior as discussed in the text which yields energy gaps $\Delta_{T_1} = 251.3 \pm 49.4$ meV and $\delta = 1.8 \pm 2.4$ meV. The external field was adjusted (from 8.5900 T at 5 K to 8.5455 T at 300 K) such that the observed frequency was $f_0 = 19.465$ MHz for all temperatures. The inset shows the field dependence of T_1^{-1} at $T = 5$ K indicating the suppression of in-gap states with applied external field.

We assume a simplified model of the density of states (equivalent to that of Caldwell *et al.* [40]) given by,

$$\begin{aligned} \rho(E) &= \rho_i(T) \quad \text{for } \delta < |E| < W_i \\ &= \rho \text{ for } \Delta < |E| < W, \end{aligned} \tag{4}$$

and zero otherwise as shown in the inset of Fig. 3(a). We perform least-squares fits using a Levenberg-Marquardt minimization algorithm, which iteratively recalculates the model function via numerical integration of Eqs. (2) and (3) (see Supplemental Material for a full description of the curve fitting [34]). The energy gap extracted from the Knight shift $\Delta_K = 155.6 \pm 11.0$. For the Knight shift we find no indication of the presence of in-gap states, that is $\rho_i(T) = 0$, similar to the static susceptibility of SmB_6 [40]. The dominant energy gap extracted from the spin-lattice relaxation $\Delta_{T_1} = 251.3 \pm 49.4$ meV. A smaller in-gap density of states $\rho_i(T) = \rho_{i0} e^{-T/T_0}$ with an energy gap $\delta = 1.8 \pm 2.4$ meV was also found to be consistent with the small low-temperature enhancement of $T_1^{-1}(T)$. The discrepancy between the static gap Δ_K and the dynamic gap Δ_{T_1} has been observed in numerous spin-gap systems [42] and is related to differences in the processes that contribute to the Knight shift and the spin-lattice relaxation. In the majority of these spin-gap systems the dynamic gap $\Delta_{T_1} > \Delta_K$ and on average $\Delta_{T_1}/\Delta_K = 1.73$. In the case of PuB_4 we find $\Delta_{T_1}/\Delta_K = 1.6 \pm 0.3$.

While NMR is not sensitive to the surface states in bulk powders or single crystals [43], it is a powerful microscopic probe of the bulk properties of topological materials. Our ^{239}Pu NMR results are consistent with a bulk gap, which is only slightly suppressed from the DFT+SOC calculated value of 254 meV. In addition to the dominant gaplike behavior evidenced by $K_c(T)$ and $T_1^{-1}(T)$, we also find a small peak at low temperature that is reminiscent of the ^{11}B $T_1^{-1}(T)$ in SmB_6 [39] and YbB_{12} [33]. In SmB_6 the peak is thought to be due to bulk magnetic in-gap states, and while the nature of these states is still controversial, it has been suggested that these states are identical to the topologically protected surface states [6]. In PuB_4 we find that $T_1^{-1}(T = 5\,\text{K})$ is strongly field dependent as shown in the inset of Fig. 3(b), which is similar to previous field-dependent measurements of SmB_6 [40].

These results motivate further investigation of the field and Pu-substitution dependence of T_1^{-1} over a wide temperature range. Previous transport measurements find a much smaller gap $\Delta = 35$ meV [19]. This is also the case in YbB_{12}, where NMR finds a larger gap than resistivity, and may be related to the presence of in-gap states, which account for the low-temperature enhancement in T_1^{-1}. This discrepancy motivates Hall coefficient measurements in PuB_4 (which in YbB_{12} agree with the NMR-measured gap), as well as surface-sensitive tunneling or spin-polarized ARPES measurements. Finally, we note that measurements comparing ^{11}B and ^{10}B T_1^{-1} in YbB_{12} and $Yb_{0.99}Lu_{0.01}B_{12}$ provide evidence for another interpretation of the low-temperature relaxation enhancement, namely that it may be driven by fluctuations of defect-induced magnetic centers and spin-diffusion-assisted relaxation [44]. These YbB_{12} results motivate further measurements and comparison of ^{11}B and ^{10}B T_1^{-1} in PuB_4.

To conclude, we have performed ^{239}Pu NMR measurements for the second time ever in powdered and single-crystalline PuB_4. We extracted the isotropic and anisotropic shifts from the uniaxially symmetric powder pattern and demonstrate that one can observe the ^{239}Pu NMR signal in anisotropic environments and up to room temperature. The large contrast of the orbital shift between the purely ionic insulator PuO_2 ($\sim$+24.7%) and band insulator PuB_4 ($\sim$−0.5%) provide us with a new tool to investigate the nature of the chemical bond based on the value of the ^{239}Pu shift. Single-crystal ^{239}Pu NMR measurements of $K_c(T)$ and $T_1^{-1}(T)$ provide unique access to bulk gaplike behavior with an energy gap that is only slightly suppressed with respect to DFT+SOC calculations, and $T_1^{-1}(T)$ also evidences the existence of bulk in-gap states. Our confirmation of a bulk gap motivate future surface sensitive measurements to confirm the theoretical prediction that PuB_4 is a topological insulator.

The authors would like to thank D. L. Clark, Z. Fisk, P. F. S. Rosa, A. M. Mounce, S. Seo, R. Movshovich, M. Janoschek, D.-Y. Kim, D. Fobes, N. Sung, N. Leon-Brito, M. W. Malone, H.-J. Grafe, M. Požek, D. Kasinathan, and P. Coleman for stimulating discussions. Work at Los Alamos National

Laboratory was performed with the support of the Los Alamos LDRD program. T.E.A.-S. was supported as part of the Center for Actinide Science and Technology (CAST), an Energy Frontier Research Center funded by the U.S. Department of Energy, Office of Science, Basic Energy Sciences under Award No. DE-SC0016568. H.S. was also partly supported by JSPS KAKENHI Grant No. JP16KK0106. A.P.D. acknowledges the support of a Director's Postdoctoral Fellowship through the Los Alamos LDRD program.

[1] M. Z. Hasan and C. L. Kane, Colloquium: Topological insulators, Rev. Mod. Phys. **82**, 3045 (2010).
[2] X.-L. Qi and S.-C. Zhang, Topological insulators and superconductors, Rev. Mod. Phys. **83**, 1057 (2011).
[3] P. Coleman, Heavy Fermions: Electrons at the edge of magnetism, in *Handbook of Magnetism and Advanced Magnetic Materials: Fundamentals and Theory*, edited by H. Kronmüller and S. Parkin (J. Wiley and Sons, New York, 2007), pp. 95–148.
[4] M. Dzero, K. Sun, V. Galitski, and P. Coleman, Topological Kondo Insulators, Phys. Rev. Lett. **104**, 106408 (2010).
[5] M. Dzero, J. Xia, V. Galitski, and P. Coleman, Topological kondo insulators, Annu. Rev. Condens. Matter Phys. **7**, 249 (2015).
[6] T. Takimoto, SmB_6: A promising candidate for a topological insulator, J. Phys. Soc. Jpn. **80**, 123710 (2011).
[7] D. J. Kim, S. Thomas, T. Grant, J. Botimer, Z. Fisk, and J. Xia, Surface hall effect and nonlocal transport in SmB_6: Evidence for surface conduction, Sci. Rep. **3**, 3150 (2013).
[8] M. Neupane, N. Alidoust, S.-Y. Xu, T. Kondo, Y. Ishida, D. J. Kim, C. Liu, I. Belopolski, Y. J. Jo, T.-R. Chang, H.-T. Jeng, T. Durakiewicz, L. Balicas, H. Lin, A. Bansil, S. Shin, Z. Fisk, and M. Z. Hasan, Surface electronic structure of the topological kondo-insulator candidate correlated electron system SmB_6, Nature Commun. **4**, 2991 (2013).
[9] J. Jiang, S. Li, T. Zhang, Z. Sun, F. Chen, Z. R. Ye, M. Xu, Q. Q. Ge, S. Y. Tan, X. H. Niu, M. Xia, B. P. Xie, Y. F. Li, X. H. Chen, H. H. Wen, and D. L. Feng, Observation of possible topological in-gap surface states in the kondo insulator SmB_6 by photoemission, Nature Commun. **4**, 3010 (2013).
[10] K. T. Moore and G. van der Laan, Nature of the $5f$ states in actinide metals, Rev. Mod. Phys. **81**, 235 (2009).
[11] D. L. Clark, The chemical complexities of plutonium, Los Alamos Sci. **26**, 364 (2000).
[12] X. Deng, K. Haule, and G. Kotliar, Plutonium Hexaboride is a Correlated Topological Insulator, Phys. Rev. Lett. **111**, 176404 (2013).
[13] J. H. Shim, K. Haule, and G. Kotliar, Fluctuating valence in a correlated solid and the anomalous properties of δ-plutonium, Nature (London) **446**, 513 (2007).
[14] M. Janoschek, P. Das, B. Chakrabarti, D. L. Abernathy, M. D. Lumsden, J. M. Lawrence, J. D. Thompson, G. H. Lander, J. N. Mitchell, S. Richmond, M. Ramos, F. Trouw, J.-X. Zhu, K. Haule, G. Kotliar, and E. D. Bauer, The valence-fluctuating ground state of plutonium, Sci. Adv. **1**, e1500188 (2015).
[15] D. L. Clark, S. S. Hecker, G. D. Jarvinen, and M. P. Neu, Plutonium, in *The Chemistry of the Actinide and Transactinide Elements* (Springer, Dordrecht, 2006), pp. 813–1264.
[16] J. C. Lashley, A. Lawson, R. J. McQueeney, and G. H. Lander, Absence of magnetic moments in plutonium, Phys. Rev. B **72**, 054416 (2005).
[17] E. D. Bauer and J. D. Thompson, Plutonium-Based Heavy-Fermion Systems, Annu. Rev. Condens. Matter Phys. **6**, 137 (2015).
[18] X. Zhang, H. Zhang, J. Wang, C. Felser, and S.-C. Zhang, Actinide topological insulator materials with strong interaction, Science **335**, 1464 (2012).
[19] H. Choi, W. Zhu, S. K. Cary, L. E. Winter, Z. Huang, R. D. McDonald, V. Mocko, B. L. Scott, P. H. Tobash, J. D. Thompson, S. A. Kozimor, E. D. Bauer, J.-X. Zhu, and F. Ronning, Experimental and theoretical study of topology and electronic correlations in PuB_4, Phys. Rev. B **97**, 201114 (2018).
[20] J. C. Cooley, M. C. Aronson, Z. Fisk, and P. C. Canfield, SmB_6: Kondo Insulator or Exotic Metal? Phys. Rev. Lett. **74**, 1629 (1995).
[21] B. J. McDonald and W. I. Stuart, The crystal structure of some plutonium borides, Acta Crystallogr. **13**, 447 (1960).
[22] H. A. Eick, Plutonium borides, Inorg. Chem. **4**, 1237 (1965).
[23] P. Rogl and P. E. Potter, The B-Pu (boron-plutonium) system, J. Phase Equilib. **18**, 467 (1997).
[24] J. L. Smith and H. H. Hill, Magnetism in neptunium borides, in *Magnetism and Magnetic Materials-1974: 20th Annual Conference, San Francisco*, AIP Conf. Proc. 24 (AIP, Melville, NY, 1975), pp. 382–383.
[25] K. Momma and F. Izumi, VESTA 3 for three-dimensional visualization of crystal, volumetric and morphology data, J. Appl. Crystallogr. **44**, 1272 (2011).
[26] C. P. Slichter, *Principles of Magnetic Resonance*, Springer series in solid-state sciences (Springer-Verlag, Berlin, 1990).
[27] N. J. Curro, Nuclear magnetic resonance in Kondo lattice systems, Rep. Prog. Phys. **79**, 064501 (2016).
[28] A. W. Kinross, M. Fu, T. J. Munsie, H. A. Dabkowska, G. M. Luke, S. Sachdev, and T. Imai, Evolution of Quantum Fluctuations Near the Quantum Critical Point of the Transverse Field Ising Chain System $CoNb_2O_6$, Phys. Rev. X **4**, 031008 (2014).
[29] S. E. Ashbrook, J. M. Griffin, and K. E. Johnston, Recent Advances in Solid-State Nuclear Magnetic Resonance Spectroscopy, Annu. Rev. Anal. Chem. **11**, 485 (2018).
[30] J. Butterworth, The nuclear magnetic moment of plutonium-239, Philos. Mag. **3**, 1053 (1958).
[31] H. Yasuoka, G. Koutroulakis, H. Chudo, S. Richmond, D. K. Veirs, A. I. Smith, E. D. Bauer, J. D. Thompson, G. D. Jarvinen, and D. L. Clark, Observation of ^{239}Pu Nuclear Magnetic Resonance, Science **336**, 901 (2012).
[32] K. Ikushima, S. Tsutsui, Y. Haga, H. Yasuoka, R. E. Walstedt, N. M. Masaki, A. Nakamura, S. Nasu, and Y. Ōnuki, First-order phase transition in UO_2 : ^{235}U and ^{17}O NMR study, Phys. Rev. B **63**, 104404 (2001).
[33] K. Ikushima, Y. Kato, M. Takigawa, F. Iga, S. Hiura, and T. Takabatake, ^{171}Yb NMR in the Kondo semiconductor YbB_{12}, Physica B: Cond. Mat. **281–282**, 274 (2000).

[34] See Supplemental Material at http://link.aps.org/supplemental/10.1103/PhysRevB.99.035104 for further information including experimental and theoretical methods, control experiment, ^{239}Pu hyperfine coupling analysis, ^{239}Pu gap fitting procedure, ^{239}Pu spin-lattice relaxation rate anisotropy, and ^{11}B powder NMR results. The Supplemental Material includes references [24,31,37,40,45–53].

[35] C.-H. Yee, G. Kotliar, and K. Haule, Valence fluctuations and quasiparticle multiplets in plutonium chalcogenides and pnictides, Phys. Rev. B **81**, 035105 (2010).

[36] J.-X. Zhu, R. C. Albers, K. Haule, G. Kotliar, and J. M. Wills, Site-selective electronic correlation in α-plutonium metal, Nature Commun. **4**, 2644 (2013).

[37] D. C. Johnston, Stretched exponential relaxation arising from a continuous sum of exponential decays, Phys. Rev. B **74**, 184430 (2006).

[38] C. H. Booth, Y. Jiang, S. A. Medling, D. L. Wang, A. L. Costello, D. S. Schwartz, J. N. Mitchell, P. H. Tobash, E. D. Bauer, S. K. McCall, M. A. Wall, and P. G. Allen, Self-irradiation damage to the local structure of plutonium and plutonium intermetallics, J. Appl. Phys. **113**, 093502 (2013).

[39] M. Takigawa, H. Yasuoka, Y. Kitaoka, T. Tanaka, H. Nozaki, and Y. Ishizawa, NMR Study of a Valence Fluctuating Compound SmB_6, J. Phys. Soc. Jpn. **50**, 2525 (1981).

[40] T. Caldwell, A. P. Reyes, W. G. Moulton, P. L. Kuhns, M. J. R. Hoch, P. Schlottmann, and Z. Fisk, High-field suppression of in-gap states in the Kondo insulator SmB_6, Phys. Rev. B **75**, 075106 (2007).

[41] A. P. Reyes, R. H. Heffner, P. C. Canfield, J. D. Thompson, and Z. Fisk, ^{209}Bi NMR and NQR investigation of the small-gap semiconductor $Ce_3Bi_4Pt_3$, Phys. Rev. B **49**, 16321 (1994).

[42] Y. Itoh and H. Yasuoka, Interrelation between Dynamical and Static Spin Gaps in Quantum Spin Systems, J. Phys. Soc. Jpn. **66**, 334 (1997).

[43] D. Koumoulis, T. C. Chasapis, R. E. Taylor, M. P. Lake, D. King, N. N. Jarenwattananon, G. A. Fiete, M. G. Kanatzidis, and L.-S. Bouchard, NMR Probe of Metallic States in Nanoscale Topological Insulators, Phys. Rev. Lett. **110**, 026602 (2013).

[44] N. Shishiuchi, Y. Kato, O. M. Vyaselev, M. Takigawa, S. Hiura, F. Iga, and T. Takabatake, Defect-induced magnetic fluctuations in YbB_{12}, J. Phys. Chem. Solids **63**, 1231 (2002).

[45] K. Schwarz and P. Blaha, Solid state calculations using WIEN2k, Comput. Mater. Sci. **28**, 259 (2003).

[46] J. P. Perdew, K. Burke, and M. Ernzerhof, Generalized Gradient Approximation Made Simple, Phys. Rev. Lett. **77**, 3865 (1996).

[47] P. Blaha, K. Schwarz, and P. Herzig, First-Principles Calculation of the Electric Field Gradient of Li_3N, Phys. Rev. Lett. **54**, 1192 (1985).

[48] G. Kotliar, S. Y. Savrasov, K. Haule, V. S. Oudovenko, O. Parcollet, and C. A. Marianetti, Electronic structure calculations with dynamical mean-field theory, Rev. Mod. Phys. **78**, 865 (2006).

[49] K. Haule, C.-H. Yee, and K. Kim, Dynamical mean-field theory within the full-potential methods: Electronic structure of $CeIrIn_5$, $CeCoIn_5$, and $CeRhIn_5$, Phys. Rev. B **81**, 195107 (2010).

[50] P. Werner and A. J. Millis, Hybridization expansion impurity solver: General formulation and application to Kondo lattice and two-orbital models, Phys. Rev. B **74**, 155107 (2006).

[51] K. Haule, Quantum monte carlo impurity solver for cluster dynamical mean-field theory and electronic structure calculations with adjustable cluster base, Phys. Rev. B **75**, 155113 (2007).

[52] D. M. Nisson and N. J. Curro, Nuclear magnetic resonance Knight shifts in the presence of strong spin-orbit and crystal-field potentials, New J. Phys. **18**, 073041 (2016).

[53] R. K. Harris, E. D. Becker, S. M. Cabral De Menezes, R. Goodfellow, and P. Granger, NMR nomenclature. Nuclear spin properties and conventions for chemical shifts (IUPAC Recommendations 2001), Pure Appl. Chem. **73**, 1795 (2001).